International Journal of Advanced Trends in Engineering and Management (IJATEM)
Vol. 1(03), August 2022, pp. 11-20

A Fast and Accurate Estimation of Channel Availability Using Hilbert Transform and Hybrid Ml-MMSE Equalizer

C. Abitha[1], S. Abisha [2]

[1]Communication System, Rohini College of Engineering and Technology, Kanyakumari, India.

[2]Associate Professor, Communication System, Rohini College of Engineering and Technology, Kanyakumari, India.

ABSTRACT

This project proposes a fast and accurate estimation of channel availability using Hilbert transform and hybrid ML-MMSE equalizer. Large-scale multi-input, multi-output orthogonal frequency division multiplexing (MIMO-OFDM) systems for the uplink, an effective channel estimation method is used. Hilbert transform is a simple technique and using this the complexity of the overall process is minimized. An effective hybrid minimal mean square error (ML-MMSE) equalizer is utilized to estimate channel availability accurately. The proposed approach is evaluated using MATLAB simulation.

1 Introduction

Multiple access passive optical networks (PONs) would produce forward signals maximum power ratios that are less than 2 dB lower than those generated with OFDM and the DFT there for converging 5G networks [1]. The suggested technique uses configurable and adaptive digital filters to multiplex multiple independent OFDM channels which integrated in ONU simultaneous retrieval in the OLT by a single FFT operation, thereby reducing overall filter DSP complexity and enhancing the adaptability and robustness of hybrid OFDM-DFMA PONs [2]. Timing jitter analysis and reduction for hybrid OFDM-DFMA PONs may be done efficiently and economically with the help of this technology [3]. With Spectrally Overlapping Digital Orthogonal Filters and Multiple Access PONs, one transmission's capacity has risen and performance has improved by about 18% [4]. It has been shown that OFDM-Digital Filter Hybrid Multiple Access PONs may deliver combined raw 30Gbit/s over 25km upstream broadcasts while degrading receiver sensitivity by 1 dB (2.5 dB) [5]. Massive MIMO is made possible by in-phase and quadrature-phase imbalances channel estimates under the less stringent limitation [6].

The clipping-enhanced optical OFDM method for VLC systems sends data via additional time slots that permit a higher modulation index in order to improve the signal-to-noise ratio and lessen clipping distortion caused by peak power constraints [7]. An All-Silicon 100-G-Baud 32 QAM Transmitter's Pre-Equalization and Bandwidth Limitation, It lowers the Tx optical power while raising the signal's peak to average power ratio [8]. Using online extreme learning machines, channel estimates and equalizations for OFDM systems with extraordinary resilience [9]. With low-resolution ADCs, this permits steady communication and massive MIMO uplink [10]. One-bit ADCs are used in large-scale MIMO systems, and studies of the channel capacity of single-carrier and OFDM distribution show that it is effective in this setting [11]. Receiving Energy Efficiency and Frequency Level Design have been shown to lower the energy burden for Massive MIMO Uplink with Mixed ADC [12]. One-bit MIMO systems with multiuser identification may require less base station power (BS) [13]. The performance evaluation method is called Bayesian Optimal Data Detector for Hybrid Millimeter Wave MIMO-OFDM Systems with Low-Resolution ADCs [14]. By utilizing spatial multiplexing and the vast bandwidths present in mm Wave frequency bands, millimeter wave (mm Wave) communication with antenna array-and-beam forming has been viewed as a potential technology for contemporary communication systems.

2 Proposed System

2.1 Transmitter

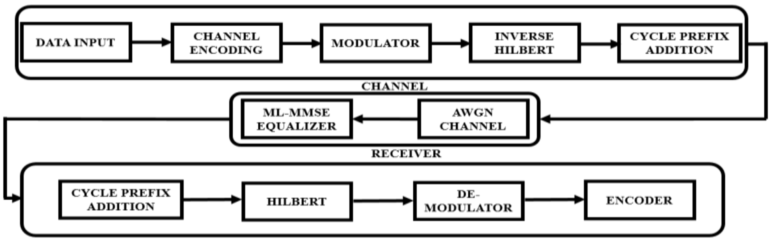

Figure: 2.1: *Proposed block diagram*

The estimated coefficients of the effective channels serve as the foundation for the study's prototype phase shift scheduling technique. As a result of APSPs may cause the channel estimation to perform poorly, create a channel estimation error-resistant data detection method based on the ML-MMSE criterion. The recommended solution can simultaneously address IQI and pilot interference. For ML-MMSE channel estimation, which is based on a real-valued mode, no additional resources are required. The Hilbert and Inverse Hilbert simple processes, respectively, can effectively translate signals from the time time domain to the frequency and from the frequency domain into the time domain. The interference between the real and fictitious components utilizing the wireless channel as the effective channel and the output of the IQI matrix results in the IQI impact. Operator-valued free probability theory can be used to calculate an asymptotic deterministic approximations for the ergodic feasible sum rate of the proposed detection method.

2.2 Massive Mimo-Ofdm Channel Model

Utilizing a robust, physically supported MIMO-OFDM channel model, analyse an intrinsic channel sparseness feature. Imagine a wireless network with a single cell, TDD wideband massive MIMO, one BS with M antennas, and K single-antenna nodes UTs. K = 0–1 is the designation for the UT set, where K stands for the UT index. Consider each channel from different UTs is independent. Consider the base station contains a uniform linear array with antennas spacing half a wavelength apart. The response vector for the BS array is then provided for the incidence angle relative to the array's perpendicular.

$$v_{M,\theta} = [\ 1\ \exp(-\jmath\bar{\pi}\ \sin(\theta)) \ldots \ldots \exp(-\jmath\bar{\pi}\ (M-1)\sin(\theta))]^T \in \mathbb{C}^{M\times 1} \quad (1)$$

Since directional antennas can be used at the BS to confine the signals seen there to lie in the angle interval A = [/2, /2], for incidence angles / A, it is pre summated that the BS receives no signals. As a result, for these angles, the BS exhibits no signals.

We take into account Nc-point inverse DFT-based OFDM modulation with Nc subcarriers, along with a guard interval of length Ng (Nc) samples. We use Tsym = (Nc + Ng) Ts and Tc = NcTs, respectively, to describe the length of an OFDM symbol with and without a guard interval. Ts is the length of the system sampling. Length of the guard interval Tg = NgTs is larger than the total maximum channel latency of all UTs, as pre summated.

The channels change from one OFDM symbol to the next while remaining constant during one OFDM signal. We write [gk,l,n]m to represent the uplink (UL) channel gain between the kth UT and the mth BS antenna over the OFDM symbol l and subcarrier n. The channel response vector gk,l,n CM1 can be characterized as follows using a physical channel modelling strategy:

$$g_{k,\ell,n} = \sum_{g=0}^{Ng-1} \int_{-\infty}^{\infty} \int_{-\pi/2}^{\pi/2} v_{M,\theta} \cdot \exp\left(-\bar{\jmath}2\pi \frac{n}{nTc}\tau\right) \cdot \exp(\bar{\jmath}2\pi\nu\ell T_{sym}) \cdot g_k(\theta,\tau,\nu) \cdot \delta(\tau - qT_s)\, d\theta d\nu$$

$$g_{k,\ell,n} = \sum_{g=0}^{Ng-1} \int_{-\infty}^{\infty} \int_{-\pi/2}^{\pi/2} v_{M,\theta} \cdot \exp\left(-\bar{\jmath}2\pi \frac{n}{nTc} q\right) \cdot \exp(\bar{\jmath}2\pi\nu\ell T_{sym}) \cdot g_k(\theta, qT_s, \nu)\, d\theta d\nu \quad (2)$$

gk (,, v) is the incidence delay, angle, and Doppler frequency-corresponding complex-valued joint angle-delay-Doppler channel gain function of UT k. vM, is provided in (1), and it is given as a function of the angle, delay, and ν. Note that |gk (, qTs, v)| is typically close to 0 for most q, proving that there are often fewer and smaller important channel taps than Ng in delayed domain. Use (2) to create a universal channel representation that is applicable to all UTs because positions of significant channel taps in the latency domain frequently change for various UTs.

We denote the kth UT's channel at the OFDM symbol l as overall sub carriers.

$$Gk,\ell = [g_{k,\ell,0}\quad g_{k,\ell,1}\ \ldots\ g_{k,\ell,Nc-1}] \in \mathbb{C}^{M\times Nc} \quad (3)$$

Which we'll call the space-frequency domain channel response matrix (SFCRM). It is simple to demonstrate from (4.2) that

$$\text{vec}\{G_{k,\ell}\} = \sum_{g=0}^{Ng-1} \int_{-\infty}^{\infty} \int_{-\pi/2}^{\pi/2} [f_{Nc,q} \otimes v_{M,\theta}] \cdot \exp(\bar{\jmath}2\pi\nu\ell T_{sym}) \cdot g_k(\theta, qT_s, \nu)\, d\theta d\nu \quad (4)$$

2.3 Hilbert–Huang Transform

Seismic signal analysis has made use of the Hilbert-Huang transform (HHT), which was introduced as a suitable technique for evaluating a nonlinear and non-stationary signal. HHT consists of two parts: 1) a Hilbert Transform (HT) and 2) Ensemble Empirical Mode

Decomposition (EEMD). EEMD is a technique for breaking down time-series data into intrinsic mode functions (IMFs) while taking the waveform envelope into account. The HHT proceeds as follows: 1) perform EEMD; 2) execute a HT; 3) generate the analytic signal; and 4) determine the analytic signal's instantaneous frequency and amplitude using time-series data. Therefore, the HHT can be used to analyse a nonlinear and non-stationary signal. A time series of the torque applied to an HDD carriage arm was built in this work using a finite element (FE) analysis. The time series was next subjected to the HHT. At last, outcomes of the Fourier transform (FT) and the HHT were contrasted.

2.4 Pilot Phase Shift Scheduling

Massive MIMO-OFDM with APSPs channel prediction and estimation was examined and identified that the optimum pilot phase shift scheduling condition that holds for both of these operations. Even though such an ideal situation is not always possible in reality, Phase shift scheduling for pilots is still useful. There may be different scheduling requirements. The issue can be stated as follows, for instance, if the MMSE-CE criterion is used to plan the pilot phase shifts

$$\underset{\{\phi k:k\in K\}}{\arg\min} \in^{CE} \quad (5)$$

Where $\in^{CE}$ is defined. A thorough search is required to uncover the best solutions to this combinatorial scheduling problem. Because the channel estimation and prediction optimal phase shift scheduling criteria are the same, the solution to problem (5) can likewise be predicted to perform well under the MMSE-CP standard. An efficient pilot phase shift scheduling algorithm may be created using the results of the previous subsections' channel estimation and prediction experiments, which served as the motivation. We begin by defining the function that assesses the amount of overlap between two real matrices A, B RMN.

$$\xi\,(\mathbf{A},\mathbf{B}) \cong \frac{\sum i,j\ [A \odot B]\ i,j}{\sum i,j\ [A]2i,j \cdot \sqrt{\sum}\ i,j\ [B]\ 2\ i,j} \quad (6)$$

It follows that an overlapping degree function in (6) satisfies 0 (A, B) 1 based on the Cauchy-Schwarz inequality. A is a scaled version of **B**, ξ (**A, B**) = 1. (A, B) = 0 positions of the non-zero items in A and B do not overlap. We selected a threshold in our algorithm to strike a compromise between the complexity of the algorithm and the effectiveness of the channel acquisition. Overlap function between the ADCPMs have various UTs is made significantly lower than predetermined threshold γ by organising the pilot phase shifts for various UTs. It makes intuitive sense that, despite having a more complex algorithm, channel acquisition performance will be greater as lower the threshold.

2.5 Inverse Fast Fourier Transform

The IFFT theoretically transforms input data from the frequency domain to output data from the time domain. IFFT block thus offers a simple method for modulating information into N orthogonal sub - channels. Output of the IFFT represents the sum of all N sinusoids. The output of the IFFT is a measure of the sum of all N sinusoids. Thus, the IFFT block provides a straightforward technique for modulating information among N orthogonal subcarriers. An OFDM symbol is made up of N output values from the IFFT in a block.

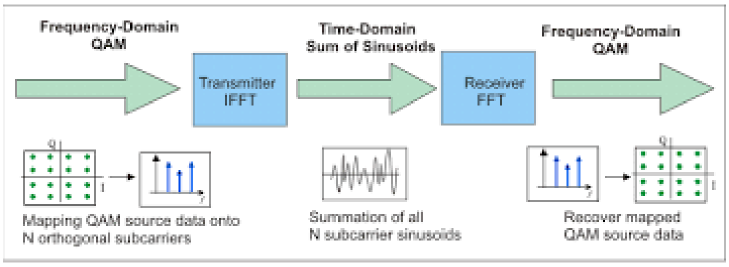

Figure 2.2: *IFFT make up a single OFDM symbol.*

2.6 Channel

An important role for channel estimation in an OFDM system. One channel is used to combine several sub-carriers on neighboring frequencies using the frequency division multiplexing technique known as OFDM. An OFDM system also uses sub-carrier overlapping to increase spectral efficiency. Normally, adjacent channels that overlap can cause interference. The steps involved are as follows. i) Use a channel matrix to establish a mathematical model correlating the "broadcast signal" with the "received signal." ii) Transmit a well-known signal (this is sometimes referred to as a "reference signal" or "pilot signal") and then listen for the response. When a channel has been equalised, the frequency domain properties of the signal at the input are properly reproduced at the output.

2.7 Receiver

The orthogonal frequency-division multiplexing (OFDM) receiver design, a method that enables the transmission of digital data across a network of carriers, is easily introduced in this helpful book.

2.7.1. Cyclic Profix Removal

Prior to transmitting the packet data to the FFT for demodulation in an OFDM receiver, the cyclic prefix is removed. In highly dynamic setups found in next-generation wireless systems, the length of the cyclic prefix varies depending on the mode, higher-level protocol and transmission frame structure.

2.7.2. Fast Fourier Transform

Sharpening edges and creating effects in static images are all common uses for the quick Fourier transform, which may also be used to transform a number series into sine waves and graphs. The discrete Fourier transform (DFT), which is how Fourier transforms are used in practice, is quickly carried out using the FFT.

2.7.3. De-Modulator

By employing an FFT operation to create N parallel data streams, an OFDM input signal is demodulated by the OFDM Demodulator System object. It starts with a bank of N correlates, one of which is allocated to each OFDM subcarrier, then it converts from parallel to serial. A system that separates the modulating signal from the carrier and recovers the modulation (data, audio, video, etc) (or carriers).

2.7.4. Decoder

The fundamental decoding component can be an AND gate because it only generates a high output when all inputs are high. The next step is to transfer the FFT output to actual data bits once we have rectified the residual CFO and the channel gain. This is the reverse encoding phase of a packet.

Demodulation: complex number to bits

- DE interleaving: each OFDM symbol's bits are randomly distributed.
- Convolution decoding: correct potential bit errors and remove redundancy
- Descramble.

After the lengthy preamble, Regardless of the actual modulation, the SIGNAL field is always BPSK modulated and is encoded in the first OFDM symbol. Remember that one OFDM symbol in 802.11a/g has 48 data sub-carriers, which are equivalent to 48 data bits in the BPSK scheme. There are 24 actual data bits in the SIGNAL field due to convolutional encoding in the SIGNAL field at a rate of 1/2.

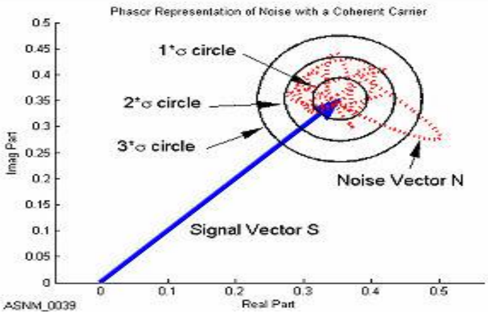

Figure 2.3: *Additive white Gaussian noise Channel*

2.7.5. ML- MMSE equalizers

Due to the characteristics of MIMO systems, large gains in data throughput and link range can be achieved without the need for extra bandwidth or transmit power. Multipath fading is the main cause of communication problems in wireless channels. Once more, the space-time pre-coding block transforms the interleaved code words into data symbols, which are then input by the symbol mapper, space-time encoder, and antenna array and detected by passing over the network. MIMO channel can be visualized as the result of the inclusion of a fixed component and a fading component when there is a LOS component between the transmitter and the receiver.

2.8 Modulator

Modern applications like high-definition video, wireless backhaul, and 5G communications all require high-speed data transport. The mm-wave band's spectrum windows can be used by the transceiver to achieve data throughput rates up to 10 Gbps. Having high data rates and excellent signal-to-noise ratios, complex modulation schemes like OFDM, 16-QAM, and 64-QAM are routinely utilized to maximize spectral efficiency (SNR). The requirement for high linearity and low phase noise in the local oscillator (LO) and mm-wave transceiver, respectively, further increases the design complexity. An ultra-linear in-phase quadrature modulator is needed to achieve the challenging digital modulation's SNR. Generally speaking, a doubly balanced diode mixer or a resistive ring mixer can be used, however they typically need more LO power.

Result And Discussion

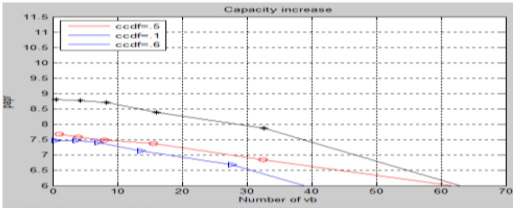

Figure 3.1: *Vector OFDM signal*

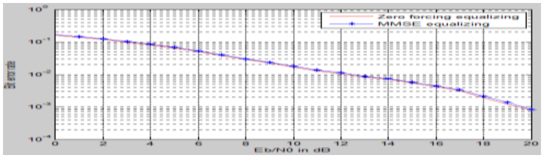

Figure 3.2: *Vector OFDM signal bit error rate during quantization*

The figure 3.1 shows the Vector OFDM quantization signal. The input from the predefined data's are loaded for Lifi Communication, the input nonlinear waveforms are varying with the help of Modulation index. By increasing the modulation index the signal noises are getting reduced. Also by changing the sub carriers (vb), the noises gets reduced. The figure 3.2 shows the bit rate error between the led communication polarizations, the proposed system reduce the error bit rates. By increasing the modulation index, error rate also reduced.

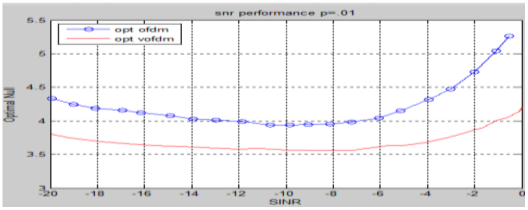

Figure 3.3: *SNR comparison of OFDM and vector OFDM with optimum error*

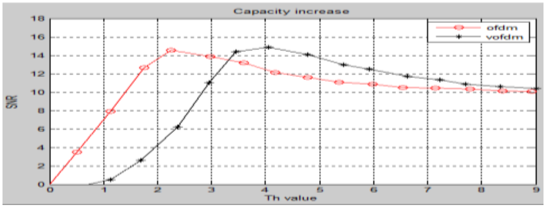

Figure 3.4: *SNR comparison of OFDM and vector OFDM*

The figure 3.3 shows the comparison between the LIFI communications with optimum techniques between the polarizations. Compared to OFDM, in vector OFDM error rate and SINR is very less. The figure 3.4 shows the SNR comparison between OFDM and vector OFDM for the proposed lifi communications, in our proposed system LIFI with vector ofdm reduces the SNR much better compared to OFDM.

Figure 3.5: *Noise level Comparison between Gabor filter and Median filter*

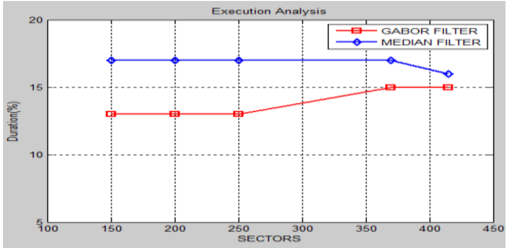

Figure 3.6: *Time Execution analysis between Gabor and median filter*

The figure 3.5 shows the error rate reduction comparison with non-Gaussian Median and Gabor filter. Gabor filter reduce the noises significantly compared to median filter. The figure 3.6 shows the time execution analysis of Gabor and median filter for time consumption analysis. The Gabor filter reduce the processing time compared to median filter.

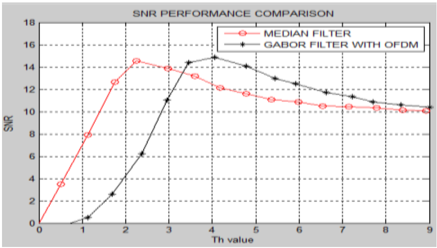

Figure 3.7: *SNR Comparison between Gabor and Median filter*

The figure 3.7 shows the SNR comparison between non Gaussian Gabor and Median filter. The Gabor filter significantly reduce the noises.

3 Conclusion

In this project, to enable rapid and precise detection of the channel by reducing the inter symbol interference (ISI) to a maximum extent. Created a data detection that is resistant to estimation error based on the acquired channel estimations. Researchers discovered an asymptotic foreseeable identical quantity for the overall feasible sum rate of the suggested detection strategy using operator valued free probability distributions. When representing the received signal with a real valued model, wireless channel and IQI are used as an effective channel. Use the Hilbert transform to lower the computational complexity of the system. The numerical results showed that the suggested channel estimation and data identification performed better when handling IQI and multi-user noise. Using a lower bit error rate, the hybrid minimal mean square error with actual values is obtained.

References

1. Y. X. Dong; W. Jin; R. P. Giddings; M. O'Sullivan; A. Tipper; T. Durrant; J. M. Tang, Year: 2019, "Hybrid DFT-Spread OFDM-Digital Filter Multiple Access PONs for Converged 5G Networks", Journal of Optical Communications and Networking, Vol.11, no.7 pp. 347 – 353.

2. Yixian Dong; Roger Philip Giddings; Jianming Tang, Year: 2018, “Hybrid OFDM-Digital Filter Multiple Access PONs”, Journal of Lightwave Technology,” Vol.36, no.23, pp. 5640 – 5649.

3. Omaro Fawzi Abdelhamid Gonem; Roger Philip Giddings; Jianming Tang, Year: 2021, “Timing Jitter Analysis and Mitigation in Hybrid OFDM-DFMA PONs”, IEEE Photonics Journal, Vol.13, no.6.

4. Abdulai Sankoh; Wei Jin; Zhuqiang Zhong; Jiaxiang He; Yanhua Hong; Roger Philip Giddings; Iestyn Pierce; Maurice O'Sullivan; Jeffrey Lee; Tim Durrant; Jianming Tang, Year: 2020, “Hybrid OFDM-Digital Filter Multiple Access PONs Utilizing Spectrally Overlapped Digital Orthogonal Filtering”, IEEE Photonics Journal, Vol.12,no.5.

5. W. Jin; Z. Q. Zhong; J. X. He; A. Sankoh; R. P. Giddings; Y. H. Hong; I. Pierce; M. O’Sullivan; C. Laperle; J. Lee; G. Mariani; T. Durrant; J. M. Tang, Year: 2020, “Experimental Demonstrations of Hybrid OFDM-Digital Filter Multiple Access PONs,” IEEE Photonics Technology Letters, Vol.32,no.13, pp. 751 – 754.

6. Z. Q. Zhong; W. Jin; S. Jiang; J. X. He; D. Chang; Y. H. Hong; R. P. Giddings; X. Q. Jin; M. O'Sullivan; T. Durrant;J. Trewern; G. Mariani; J. M. Tang, Year: 2021, “Concurrent Inter-ONU Communications for Next Generation Mobile Fronthauls Based on IMDD Hybrid SSB OFDM-DFMA PONs”, Journal of Lightwave Technology, Vol.39,no.23, pp. 1542 – 1555.

7. Yan Chen; Li You; Xiqi Gao; Xiang-Gen Xia, Year: 2020, “Channel Estimation With Pilot Reuse in IQ Imbalanced Massive MIMO”, IEEE Access, Vol.8, pp. 1542 – 1555.

8. J. Lian; M. Brandt-Pearce, Year : 2019 "Clipping-Enhanced Optical OFDM for Visible Light Communication Systems," in Journal of Lightwave Technology, Vol. 37, no. 13, pp. 3324-3332,.

9. L. Zhu; J. Zhou; J. Wang; Q. Zhang, Year: 2019 "Pre-Equalization and Bandwidth Limitation for a 100-G-Baud 32 QAM All-Silicon Transmitter," in IEEE Photonics Technology Letters, Vol. 31, no. 17, pp. 1453-1456.

10. J. Liu; K. Mei; X. Zhang; D. Ma; J. Wei, Year: 2019 "Online Extreme Learning Machine-Based Channel Estimation and Equalization for OFDM Systems," in IEEE Communications Letters, Vol. 23, no. 7, pp. 1276-1279.

11. S. Jacobsson; G. Durisi; M. Coldrey; U. Gustavsson; C. Studer, Year: 2017, “Throughput analysis of massive MIMO uplink with low-resolution ADCs,” IEEE Trans. Wireless Commun., Vol. 16, no. 6, pp. 4038-4051.

12. C. Mollen; J. Choi; E. G. Larsson; R. W. Heath, Year: 2017, “Uplink performance ´ of wideband massive MIMO with one-bit ADCs,” IEEE Trans. Wireless Commun., Vol. 16, no. 1, pp. 87-100.

13. Q. Ding; Y. Jing, Year: 2018, "Receiver energy efficiency and resolution profile design for massive MIMO uplink with mixed ADC," IEEE Trans. Veh. Tech., Vol. 67, no. 2, pp. 1840-1844.

14. P. N. Alevizos, Year: 2018, "Low-complexity multiuser QAM detection for uplink 1- bit massive MIMO," IEEE Commun. Lett., Vol. 22, no. 8, pp. 1592-1595.

15. H. He; C. K. Wen; S. Jin, Year: 2018, "Bayesian optimal data detector for hybrid mmwave MIMO-OFDM system with low-resolution ADCs," IEEE J. Sel. Areas Commun., Vol. 12, no. 3, pp. 469-483.